Available online at www.sciencedirect.com

ScienceDirect

Solar Energy 100 (2014) 31–41

SOLAR ENERGY

www.elsevier.com/locate/solener

Development of a model to simulate the performance characteristics of crystalline silicon photovoltaic modules/strings/arrays

Tao Ma *, Hongxing Yang, Lin Lu

Renewable Energy Research Group (RERG), Department of Building Services Engineering, The Hong Kong Polytechnic University, Hong Kong

Received 28 June 2013; received in revised form 6 September 2013; accepted 1 December 2013

Communicated by: Associate Editor Elias K. Stefanakos

Abstract

In this study, a novel theoretical model, offering a good compromise between accuracy and simplicity, was developed in Matlab for determining solar photovoltaic (PV) module parameters and then fitting the model to experimental *I–V* characteristic curves of a PV module/string/array. A few inputs are only needed for the model, which can be obtained from the manufacturer datasheet. With this newly developed model, the performance of a PV module/string/array at any solar irradiance and module cell temperature can be easily simulated. To validate the simulation model, the parameters from the simulation and *I–V* characteristic curves were compared with those from the DeSoto model and other simulation software (INSEL and PVsyst) at different temperature and irradiation. The comparison results present a high degree of agreement. Moreover, a series of field measurements were carried out from an existing 22 kWp grid-connected PV system located in The Hong Kong Polytechnic University to further validate the simulation results at a wide range of real operating conditions. To have more realistic results, the model was then slightly modified by including the effect of soiling, aging and other derating factors. Field test results demonstrate that the modified simulation model can accurately predict the *I–V* curve characteristics of PV modules/strings/arrays demonstrating the feasibility and reliability of the developed simulation model.

Keywords: Mathematic model; PV module/string/array; Experimental verification; Field measurement

1. Introduction

Energy is an essential component for all social activities, required for production of all goods and provision of all services (Muneer et al., 2003). At present our world is mainly powered by fossil fuels. With the wide concerns in recent years on global warming and harmful environmental effects from carbon fuels, a global movement to utilizing renewable energy, such as solar photovoltaic (PV), is therefore under way to help meet increased energy needs and carbon reduction target. As for China, the national energy administration announced that the cumulative installed solar PV capacity would increase from 3.3 GW in 2011 to 20 GW in 2015 from its 12th Five-Year Plan (Jäger-Waldau, 2012).

With the robust growth of solar PV applications, accurate prediction of the characteristic parameters of solar PV models/strings/arrays becomes an essential topic of research since it is very important to actually know the system's performance in the planning and design stages of PV systems. The designers require a reliable tool to predict PV module energy production under real conditions to make a sound decision on selection of different PV modules (Carrero et al., 2007; De Soto et al., 2006; Dongue et al., 2012). Besides, engineers also need an accurate tool to simulate the power output from a PV plant under real operating conditions for evaluating the system's energy performance. However, the specifications of a PV module from its manufacturer cannot help us to determine its

* Corresponding author. Tel.: +852 27664836; fax: +852 27657198.
E-mail address: Tao.Ma@connect.polyu.hk (T. Ma).

0038-092X/$ - see front matter © 2013 Elsevier Ltd. All rights reserved.
http://dx.doi.org/10.1016/j.solener.2013.12.003

power production in real conditions, since the specifications are obtained at standard test condition (STC): incident sunlight of 1000 W/m^2, a cell temperature of 25 °C and an air mass of 1.5. To make them effective at other general conditions, an accurate and reliable solar PV power prediction model, therefore, is urgently needed (Lo Brano et al., 2010, 2012).

The electrical behavior of a crystalline silicon photovoltaic device is characterized by its current–voltage (*I–V*) curve. Substantial research on *I–V* curve predictions can be founded in literatures. The overview of various methods commonly used can be seen from the literatures (Ishaque and Salam, 2011; Ishaque et al., 2011a,b; Saloux et al., 2011). Among them, the most accurate model, denoted as two-diode model (Gow and Manning, 1999), uses an equivalent circuit with double diodes, while it is quite complex and computational time is long since it is a nonlinear and implicit equation with two exponential terms and up to seven unknown parameters (Ishaque et al., 2011a,b).

For simplification, the one-diode model of crystalline silicon modules is usually employed in literatures, based on the assumption that the recombination loss in the depletion region is absent (Ishaque et al., 2011a). The single diode models can be further divided in to two categories. If the shunt resistance is considered as infinite, it is the so-called four-parameter model (Mellit et al., 2007). However, Dongue et al. (2012) reported that the four-parameter model that neglects the effects of the shunt resistance was inadequate to fit experimental *I–V* and *P–V* data in current-source operation.

To have a more accurate result but not to complicate the calculation, the five-parameter model based on the one-diode equation is put forward. The complete five-parameter model (Karatepe et al., 2006; Lo Brano et al., 2010, 2012; Sera et al., 2007; Tian et al., 2012) consists of photo-generated current, diode reverse saturation-current, series resistance, shunt resistance and diode ideality factor of PV modules. The five-parameter developed by De Soto et al. (2006) can accurately simulate the *I–V* characteristics, while the ideality factor calculated from this model is usually less than one, not within the reasonable range.

Apart from the diode based model, the model developed by Sandia National Laboratory (King et al., 2004) can accurately predict the power production of crystalline silicon PV modules, but it requires some inputs that are not normally available from manufacturers. Some other models that describe the behavior of a photovoltaic module or the energy produced from it, based on empirical approaches, are studied elsewhere (Durisch et al., 2000; Meyer and van Dyk, 2000). In addition, some commercial software, such as TRNSYS, PVsyst, Simulink and INSEL, also has the PV performance simulation function for users to easily understand PV module operating performance. Unfortunately, these models are too general and the results are not so accurate, so that they are not suitable for particular PV modules.

In this study, a novel theoretical model was developed in the Matlab environment to determine PV module's parameters and then fit the model to experimental *I–V* characteristic curves obtained from real PV systems, especially at the vicinities of characteristic points: the short circuit (0, I_{sc}), maximum power point (MPP) (V_{mp}, I_{mp}), and open circuit (V_{oc}, 0) of a PV module. Only a few inputs are needed for this model and all of them can be directly obtained from the manufacturer datasheet. This model offers a good compromise between simplicity and accuracy. With this newly developed model, the electrical parameters of a PV module or PV array can be easily obtained and the performance of a PV module or PV array under any weather conditions can be simulated. If a model is able to accurately represent the entire *I–V* characteristics, it will be suitable for any general purpose.

2. Simulation model

A solar cell is traditionally represented by an equivalent circuit composed of a current source, a diode (*D*), a shunt/parallel resistance (R_p) and a series resistance (R_s). As shown in Fig. 1, available electrical power from the solar cell is modeled with this well-known equivalent circuit.

The photovoltaic generator is neither a constant voltage source nor a current source. It is modeled and described by the relationship between current and voltage. Based on Shockley diode equation, the mathematical model (*I–V* characteristic) for an individual PV cell is as follows (Benlarbi et al., 2004; Gow and Manning, 1999; Hadj Arab et al., 2004; Sera et al., 2007):

$$I = I_{ph} - I_D - I_p = I_{ph} - I_0\left(e^{\frac{V+IR_s}{V_t}} - 1\right) - \frac{V + IR_s}{R_p} \tag{1}$$

where I_{ph} is the photo current (A); I_0 is the diode saturation current (A); R_s is the series resistance (Ω); R_p is the shunt/parallel resistance (Ω); $V_t = \frac{nKT}{q}$ is the diode thermal voltage; n is the diode ideality factor; q is the charge of the electron (1.602E−19 Coulomb); K is the Bolzmann's constant (1.381E−23 J/K) and T is the temperature of solar cell (K). Eq. (1) presents that a solar cell is a nonlinear power source. Determination of an analytical solution of the implicit equation is a difficult and challenging work. Therefore, its numerical solution is employed in the present study.

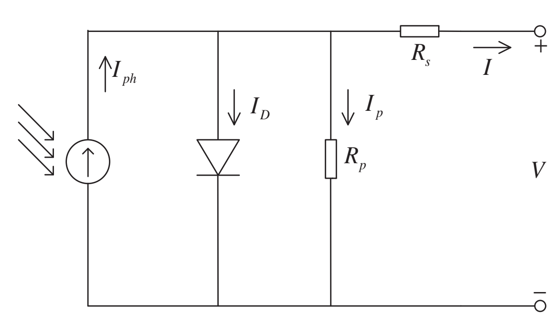

Fig. 1. Equivalent circuit for a solar cell.

This equivalent circuit can not only be used for an individual solar cell, but for a PV module with many cells, or for an array/string including dozens of modules. Therefore, the mathematical model for a PV module's power output could be deduced:

$$I = I_{ph} - I_0\left(e^{\frac{1}{V_t}\left(\frac{V_M}{N_s}+I_M R_s\right)} - 1\right) - \frac{1}{R_p}\left(\frac{V_M}{N_s} + I_M R_s\right) \tag{2}$$

where N_s represents the number of series connected cells in each module. Based on the PV module mathematic model, the output current I_A and output voltage V_A of a PV array with N_s cells in series and N_p strings in parallel can be found.

$$I = N_p I_{ph} - N_p I_0\left(e^{\frac{1}{V_t}\left(\frac{V_A}{N_s}+\frac{I_A}{N_p}R_s\right)} - 1\right) - \frac{N_p}{R_p}\left(\frac{V_A}{N_s} + \frac{I_A}{N_p}R_s\right) \tag{3}$$

This equation can be expanded to any number of solar cells in series (N_S), and thus is not restricted to one module. Therefore, for the array with N_M modules connected in series and N_C cells in series for each module, the N_S in above equation becomes $N_M \times N_C$.

From above analysis, the PV cell/module/array mathematical models are very similar. These models could be directly developed in Matlab/Simulink and other electromagnetic transient simulation programs, and then the I–V curve or P–V curve can be obtained.

The PV module from Shell Solar is used as a sample in the present study. The key parameters for the three characteristic points: short circuit (0, I_{sc}), MPP (V_m, I_m), and open circuit (V_{oc}, 0) and other operating temperature coefficients are summarized in Table 1. These parameters can be easily found in the specification datasheet from the manufacturer.

3. Parameters determination and calculation procedure

In Eq. (3), there are totally five unknown parameters to be determined: I_{ph}, I_o, V_t, R_s and R_p. The objective of this research is to solve the five parameters through the product's datasheet provided by its manufacturer. To find the five parameters, at least five equations are needed. Equations used for parameter determination are described as follows, which are generally based on the three characteristic points under STC.

Table 1
The key specifications of the Shell Solar SQ175-PC PV module.

Characteristics	Value
Open-Circuit Voltage (V_{oc})	44.6 V
Voltage at maximum power point (V_{mp})	35.4 V
Short-Circuit Current (I_{sc})	5.43 A
Current at maximum power point (I_{mp})	4.95 A
Maximum Power at STC (Pmax)	175 Wp
Number of cells connected in series	72
Temperature coefficient of I_{sc} (alpha)	0.8 mA/°C
Temperature coefficient of V_{oc} (beta)	−145 mV/°C
Temperature coefficient of Pmpp (gamma)	−0.43%/°C

(1) For an open circuit under the STC, i.e. $I = 0$ and $V = V_{oc}$,

$$0 = N_p I_{ph} - N_p I_0\left(e^{\frac{V_{oc}}{N_s V_t}} - 1\right) - \frac{N_p}{N_s}\frac{V_{oc}}{R_p} \tag{4}$$

(2) For a short-circuit under the STC, i.e. $V = 0$ and $I = I_{sc}$,

$$I_{sc} = N_p I_{ph} - N_p I_0\left(e^{\frac{I_{sc} R_s}{N_p V_t}} - 1\right) - \frac{I_{sc} R_s}{R_p} \tag{5}$$

(3) The maximum power point under STC, i.e. $I = I_m$ and $V = V_m$,

$$I_m = N_p I_{ph} - N_p I_0\left(e^{\frac{\frac{V_m}{N_s}+\frac{I_m}{N_p}R_s}{V_t}} - 1\right) - N_p\frac{\frac{V_m}{N_s} + \frac{I_m}{N_p}R_s}{R_p} \tag{6}$$

(4) The derivative of the power with respect to voltage is equal to zero at the maximum power point shown in Fig. 2, that is,

$$\left.\frac{dP}{dV}\right|_{P=P_m} = \left.\frac{dP}{dV}\right|_{\substack{V=V_m \\ I=I_m}} = \left.\frac{d(IV)}{dV}\right|_{\substack{V=V_m \\ I=I_m}} = I + V\frac{dI}{dV} = 0 \tag{7}$$

i.e.

$$\frac{I_m}{V_m} = -\left.\frac{dI}{dV}\right|_{\substack{V=V_m \\ I=I_m}} \tag{8}$$

Eq. (3) is a transcendent equation, which needs numerical methods to express the current and voltage. Therefore, it is rewritten as:

$$I = f(I, V) \tag{9}$$

By differentiating Eq. (9), the following equation can be obtained:

$$dI = df(I,V) = dI\frac{\partial f(I,V)}{\partial I} + dV\frac{\partial f(I,V)}{\partial V} \tag{10}$$

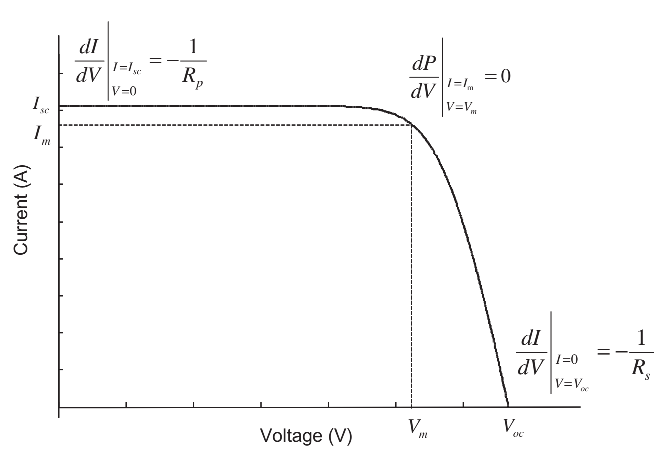

Fig. 2. The relationship between I–V curve, R_s and R_p.

Therefore:

$$\frac{dI}{dV} = \frac{\frac{\partial f(I,V)}{\partial V}}{1 - \frac{\partial f(I,V)}{\partial I}} \tag{11}$$

Substituting Eq. (11) into Eq. (8), we can deduce the fourth determination equation:

$$\frac{I_m}{V_m} = -\frac{dI}{dV}\bigg|_{\substack{V=V_m\\I=I_m}} = -\frac{\frac{\partial f(I,V)}{\partial V}}{1-\frac{\partial f(I,V)}{\partial I}}\Bigg|_{\substack{V=V_m\\I=I_m}}$$
$$= \frac{\frac{N_p}{N_sV_t}I_0 e^{\frac{V_m+I_m\frac{N_s}{N_p}R_s}{N_sV_t}} + \frac{1}{\frac{N_s}{N_p}R_p}}{1+\frac{R_s}{V_t}I_0 e^{\frac{V_m+I_m\frac{N_s}{N_p}R_s}{N_sV_t}} + \frac{R_s}{R_p}} \tag{12}$$

(5) At this moment there are four equations available. In the five-parameter model of a solar cell, the resistances R_p and R_s affect the slope of the *I–V* characteristic, before and after the curve "knee", respectively. Therefore, the fifth and final equation could be established from the derivative of the current with voltage at the short circuit point as shown in Fig. 2, which can be mainly determined by the parallel resistance R_p (Chan and Phang, 1987; Hadj Arab et al., 2004; Lo Brano et al., 2010; Sera et al., 2007), expressed as below:

$$\frac{dI}{dV}\bigg|_{\substack{I=I_{sc}\\V=0}} = -\frac{1}{R_p} \tag{13}$$

Eqs. (11) and (13) lead to:

$$\frac{dI}{dV}\bigg|_{\substack{I=I_{sc}\\V=0}} = \frac{\frac{\partial f(I,V)}{\partial V}}{1-\frac{\partial f(I,V)}{\partial I}}\Bigg|_{\substack{V=0\\I=I_{sc}}} = \frac{-\frac{N_p}{N_sV_t}I_0 e^{\frac{I_{sc}\frac{N_s}{N_p}R_s}{N_sV_t}} - \frac{1}{\frac{N_s}{N_p}R_p}}{1+\frac{R_s}{V_t}I_0 e^{\frac{I_{sc}\frac{N_s}{N_p}R_s}{N_sV_t}} + \frac{R_s}{R_p}} = -\frac{1}{R_p} \tag{14}$$

(6) Similarly, the reciprocal of the slopes of the *I–V* characteristic at the open circuit point is equal to the serial resistance at the STC (Hadj Arab et al., 2004; Lo Brano et al., 2010) (Fig. 2). This relationship can also be employed as the fifth equation:

$$\frac{dI}{dV}\bigg|_{\substack{I=0\\V=V_{oc}}} = \frac{-\frac{N_p}{N_sV_t}I_0 e^{\frac{V_{oc}}{N_sV_t}} - \frac{1}{\frac{N_s}{N_p}R_p}}{1+\frac{R_s}{V_t}I_0 e^{\frac{V_{oc}}{N_sV_t}} + \frac{R_s}{R_p}} = -\frac{1}{R_s} \tag{15}$$

(7) On the other hand, Tian et al. (2012) proposed another solution to develop the five equation based on the temperature coefficient of the open circuit voltage provided by the manufacturer. The V_{oc} at other operating temperature can be expressed as $V_{oc}[1+\beta_{Voc}(T-T_0)]$. Therefore,

$$0 = N_pI_{ph}(G,T) - N_pI_0(G,T)\left(e^{\frac{V_{oc}[1+\beta_{Voc}(T-T_0)]}{N_sV_t(G,T)}} - 1\right) - \frac{N_p}{N_s}\frac{V_{oc}[1+\beta_{Voc}(T-T_0)]}{R_p(G,T)} \tag{16}$$

where β_{Voc} is the temperature coefficient for V_{oc} and T_0 is the solar cell temperature under STC. By using Eq. (16), the temperature coefficient for V_{oc} can be guaranteed.

The first four equations are commonly used in literature. To determine the most suitable fifth equation, the results from several methods with different equations (Eqs. (14)–(16) and their combinations) are compared. It was found that the method combining Eqs. (14) and (16) is the best one as the result can fit the module's *I–V* characteristic at short circuit point and voltage thermal performance simultaneously. In addition, the above determination equations are transcendent and nonlinear, making it almost impossible to separate all unknowns and solve them analytically. A numerical method is therefore employed. The simultaneous equations were constructed in Matlab using the nonlinear equation solver 'fsolve', which is embedded with 'Levenberg–Marquardt (LM) algorithm (Blas et al., 2002)' and 'Gauss–Newton' algorithm. This solver can solve the six simultaneous equations with five unknown parameters with a rapid convergence. The values of the five parameters for a cell/module/array and its ideality factor are shown as in Table 2.

Table 2
Calculated parameters of PV cell/module.

	I_{ph} (A)	I_o (A)	R_s (Ω)	R_p (Ω)	V_t (V)	n
Cell	5.449	1.20E−09	0.010	2.725	0.028	1.086
Module	5.449	1.20E−09	0.700	196.200	0.028	1.086

4. Parameter analysis under general condition

Once the parameters under STC are determined by the simultaneous equations, the *I–V* characteristics of the PV cell/module/string/array at the STC can be easily obtained. Then it is necessary to generalize the model to other operating conditions with different solar irradiance and operating temperature. This section describes the temperature and irradiance dependence of the parameters.

The photo current I_{ph} can be described by:

$$I_{ph}(G,T) = I_{ph}[1+\alpha_{I_{sc}}(T-T_0)]\frac{G}{G_0} \tag{17}$$

where G and G_0 are the solar radiation intensities under real conditions/outdoor and STC, respectively; $\alpha_{I_{sc}}$ is the relative temperature coefficient of the short-circuit current (%/K), which represents the rate of change of the short-circuit current with respect to temperature (%).

It is well known that the diode saturation current is primarily proportional to temperature raised to the third power (Blas et al., 2002), and the relationship is expressed as (Celik and Acikgoz, 2007; De Soto et al., 2006; Tian et al., 2012; Walker, 2001; Zhang et al., 2000):

$$I_0 = AT^3\exp\left(\frac{-E_g}{nkT}\right) \tag{18}$$

where E_g is the band gap energy in eV, defined by Kim et al. (2009) as:

$$E_g = 1.16 - 7.02 \times 10^{-4} \times \frac{T^2}{T - 1108} \tag{19}$$

The effect of the changing ideality factor is not very significant on the curve shape, and usually higher ideality factor can slightly soften the knee of the curve. This present study considers the ideality factor is a constant value, following the method proposed by Tian et al. (2012). It means that the ideality factor would not change with respect to the operating condition. Therefore, the temperature dependence equation of the thermal voltage V_t is obtained from

$$V_t(T) = V_t \frac{T}{T_o} \tag{20}$$

The parallel/shunt resistance R_p represents the leakage current, which is lost mainly in the p–n interface of the diode and along the edges (Celik and Acikgoz, 2007). PVsyst and Blas et al. (2002) reported that the sensibility of the model to the value of the shunt resistance is minor, in view of which a fixed Rp does not affect the I–V characteristic greatly. In this study, R_p is taken as inversely proportional to the solar irradiance, which has been widely used by Lo Brano et al. (2010, 2012) and De Soto et al. (2006), while this assumption is opposite to that proposed by Tian et al. (2012).

$$R_p(G) = \frac{R_p}{G/G_0} \tag{21}$$

Celik and Acikgoz (2007), De Soto et al. (2006), Ahmad et al. (2003) and Blas et al. (2002) concluded that it was convenient to assume that the R_s is independent of incident irradiation and temperature, which could simplify the calculation process and guarantee a sufficient degree of precision. Therefore, a constant was assumed for R_s in this study.

PV module performance depends greatly on the solar cell operating temperature, and the temperature is influenced by many factors, such as solar irradiance, wind speed, ambient temperature (Almonacid et al., 2010). The relationship between the module back-surface temperature and cell temperature is simplified as (Almonacid et al., 2010; King et al., 2004):

$$T_c = T_m + \frac{G}{G_0} \Delta T \tag{22}$$

where T_c is the inside cell operating temperature in °C, T_m is the collected back-surface operating temperature of module in °C, and ΔT is a constant temperature difference between the cell and the module back surface (3 °C).

The effects of temperature and solar irradiance under general operating conditions have been discussed above. With the PV cell temperature in Eq. (22) and parameters obtained at STC in Table 2, these parameters in Eqs. 17, 18, 20, and 21 can be substituted in Eqs. (1)–(3) to obtain the I–V characteristic curves of the PV cell/module/array under any general operating conditions.

5. Simulation results from the proposed model and comparison with PVsyst, INSEL and DeSoto model

The performance of the proposed PV model under general operating conditions has been simulated, and compared with the results from the DeSoto model, PVsyst software and INSEL software. DeSoto model presented by De Soto et al. (2006) is a 5-parameter PV model, which was developed by Wisconsin Solar Energy Laboratory (SEL). This model is widely used to accurately predict the performance of cSi modules. PVsyst is an analysis software for PV system developed by the University of Geneva in Switzerland. It also employs the one-diode equivalent circuit model to calculate the performance of cSi modules. The basic parameters of the studied PV module can be found in the software database. The INSEL software from Doppelintegral GmbH in Germany is a PV system analysis program, and the characteristics of the studied module can be output directly from the software using the two-diode model.

The results from the four tools are summarized in Table 3. The INSEL software uses the two-diode model for the studied PV module (SQ175-PC), and thus it has two values for 'I_o' and 'n', but they could not be extracted directly from the software.

As can be seen from Fig. 2, the value of Rs mainly affects the slope of the I–V curve at V_{oc}. Table 3 indicates that the calculated R_s values from the simulation model in Matlab, Desoto model PVsyst and INSEL software are similar. The small difference would not influence the curves significantly. The graphics for the I–V and P–V curves in the following section will show the discrepancy vividly. Table 3 also reveals that all the methods can have similar R_p values. Except the temperature coefficient of the I_{sc} from the INSEL software, all the methods can meet the thermal performance ($\alpha_{I_{sc}}, \beta_{V_{oc}}, \gamma_{P_{mpp}}$) very well. These properties will determine the I_{sc} and V_{oc} values under different operating temperatures. However, the ideality factor from DeSoto model is less than 1. With a reasonable range

Table 3
Summary of parameter results.

Methods	I_{ph} (A)	I_o (A)	R_s (Ω)	R_p (Ω)	V_t (V)	n	Alpha_I_{sc} (mA/°C)	Beta_V_{oc} (mV/°C)	Gamma_Pmpp (%/°C)
Proposed model (present study)	5.449	1.20E−09	0.70	196.20	0.028	1.086	0.797	−145.3	−0.431
DeSoto model	5.457	4.67E−11	0.81	163.30	0.024	0.948	0.796	−145.2	−0.430
PVsyst software	5.43	2.00E−09	0.65	180.00	0.029	1.110	0.800	−144.7	−0.430
insel software	5.43	–	0.71	171.06	–	–	1.412	−144.9	–

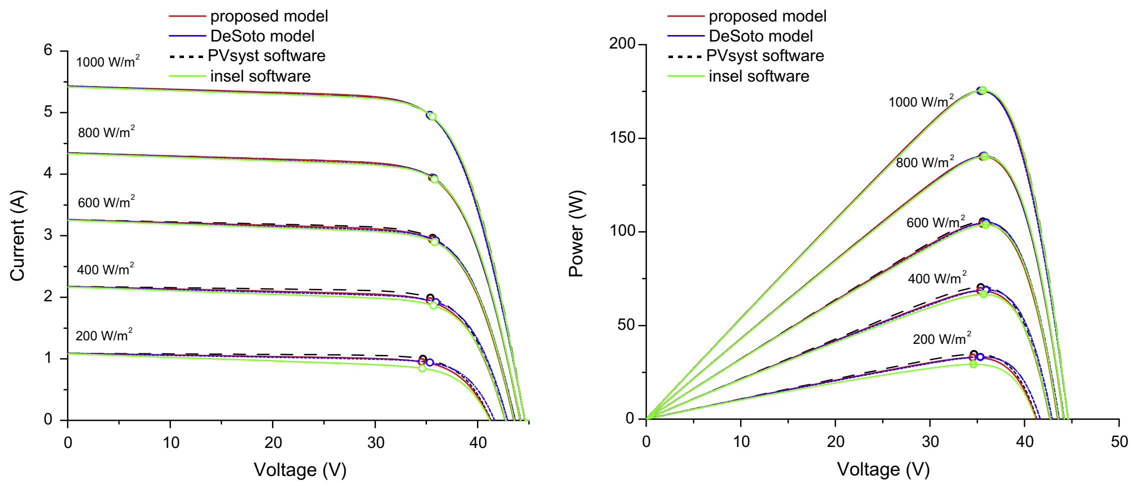

Fig. 3. I–V curves and P–V curves under different solar radiation levels (cell temperature = 25 °C).

(usually from 1 to 2), the ideality factor value determines the knee of the I–V curve near the maximum power point.

It is well acknowledged that two factors affect the PV module performance strongly: the cell temperature and the solar irradiance. Therefore, after obtaining the parameters in Table 3, the I–V characteristic curve under various irradiances and temperatures has been studied. Fig. 3 presents the I–V curves and P–V curves for solar radiation ranging from 200 W/m^2 to 1000 W/m^2 with cell temperature at 25 °C. It can be seen that the proposed model in the present study can agree well with Desoto model for the whole solar radiation range. However, discrepancy can be found from PVsyst model and INSEL model at the low solar radiation level, but it is not significant.

The I–V curves and P–V curves under different PV cell temperatures with irradiance 1000 W/m^2 are illustrated in Fig. 4. This figure presents good agreement between the results from this proposed model and that from DeSoto model and PVsyst software, especially at the three characteristic points. The relatively small deviation exists for the INSEL model due to larger temperature coefficient of I_{sc}. The graphic results show that the simulation curves from the proposed model exactly match with that from DeSoto model and PVsyst software, particularly around the maximum power point. It demonstrates that the simulation model is reliable and feasible, and therefore it could be used to characteristic the operating performance for general purpose in the future.

6. Model validation through field measurements

6.1. Experimental system

In this study, a series of outdoor measurements on a grid-connected PV system was carried out to validate the simulation results from the proposed model under different solar irradiance and temperature conditions.

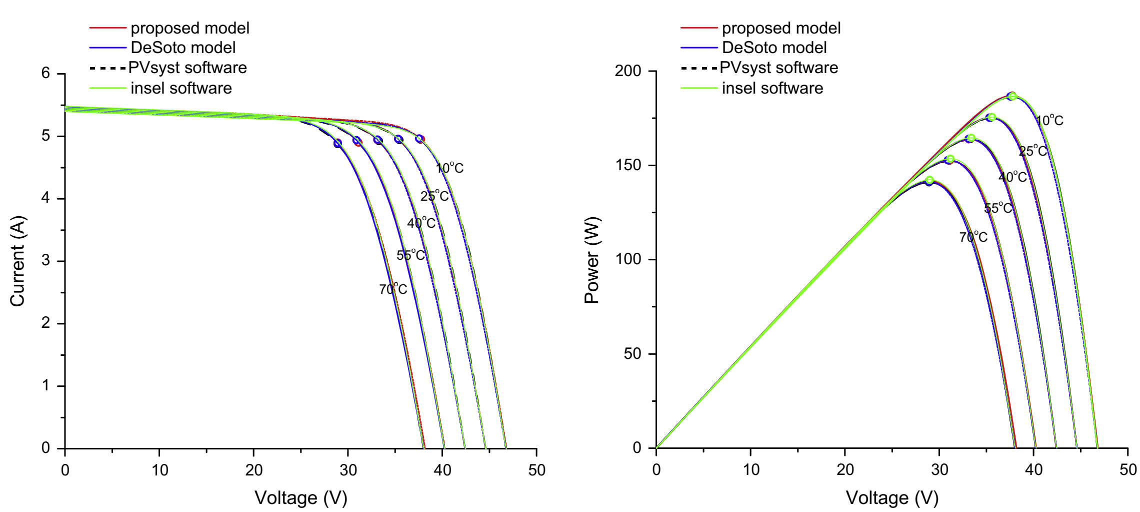

Fig. 4. I–V curves and P–V curves under different PV cell temperature levels (irradiance = 1000 W/m^2).

Fig. 5. Field measurement instruments and test rig of the 22 kWp PV system.

A portable I–V checker MP170 from EKO was employed to measure the I–V curves of the PV module/string/array. To prevent the MP170 main unit from heat generating internally, the test interval is set at 1 min. An overview of the test system is shown in Fig. 5. The output of the PV module/string/array was directly measured from the junction box attached on the back side of the module or from the subarray combiner box. To guarantee a high degree of accuracy, an external high-precision pyranometer from EKO (model: MS802; resolution: 5 μV), instead of the integrated small one, was used to measured solar radiation intensity. This method is also suggested by the manufacturer for high quality measurement. The ambient and module back temperatures were recorded by several T-type thermocouples. All these environmental data was transferred to a data logger and the sensor unit of MP170 simultaneously.

This PV system (22 kWp) locates on a rooftop on the university campus, facing south with a tilt from horizontal of 22.5°. It consists of 7 subarrays. Every array consists of 2 parallel strings with 9 PV modules linked in series. Therefore, the rated power of each array is 3150 Wp. The system's schematic diagram and tested items are illustrated in Fig. 6. Four adjacent PV modules (M1, M2, M3 and M4) were studied to compare the performance of a single module. In addition, one PV string (S1) and three PV sub arrays (A1, A2, A3) are tested.

6.2. Determination of the derating factor and modified module specification

First, the model using the specifications issued by manufacturer was used to simulate the I–V curve of the PV module at 12:46 on 22nd December 2012 with solar radiation of 820 W/m^2 and ambient temperate of 23.3 °C. It was observed that obvious discrepancy existed between the measured and simulated curve (Fig. 7), indicating that the model may not be able to accurately predict the performance of the PV system under real conditions. The similar conclusion can also be found in the literatures (Hansen et al., 2000; Tian et al., 2012). The phenomenon may results from a lot of factors, which is collectively referred to as derating factor (PVWATTS). Dust is the most significant factor because this PV system is located at a heavy traffic area, which is also related to seasonal change. In addition, weathering of the PV modules should be considered because this system has been operating for more than 6 years. Moreover, other derating factors should be taken into account, such as the degradation of manufacturer's nameplate rating when it was initially exposed to sunlight for real operations, the losses in DC wiring, voltage drop due to block diodes and shading by nearby structures. Besides, the I–V characteristics vary slightly from module-to-module.

To have a specified derating factor for this PV system, a detailed analysis was performed based on the 59 reference I–V curves of the module M1 with irradiance ranging from 200 to 900 W/m^2 and temperature from 22 to 50 °C. Since the experimental measurements have been achieved at different temperature and solar irradiance, it is necessary to translate both curves to STC conditions (Bellini et al., 2009). By complying with the IEC 60891 Standard, each current-voltage pair on the measured I–V curve was converted to a corresponding pair under STC. Therefore, the updated module's electrical specifications were obtained from the translation. The distribution of the converted specifications is presented in Fig. 8. It can be seen that the average I_{sc} at STC is 5.16 A, smaller than

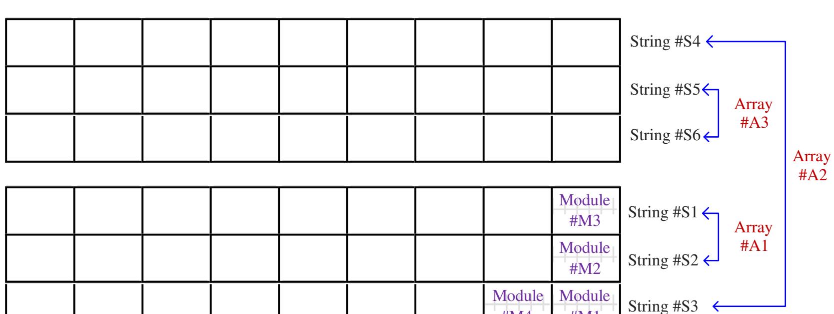

Fig. 6. PV system configuration and test items including PV modules (M1, M2, M3, M4), strings (S1, S2, S3) and arrays (A1, A2, A3).

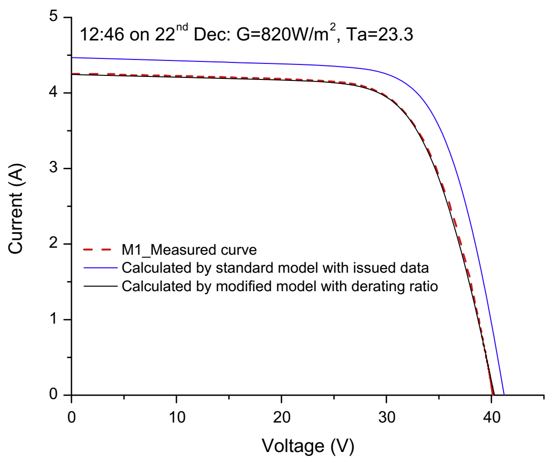

Fig. 7. The measured and calculated I–V curves of PV module M1.

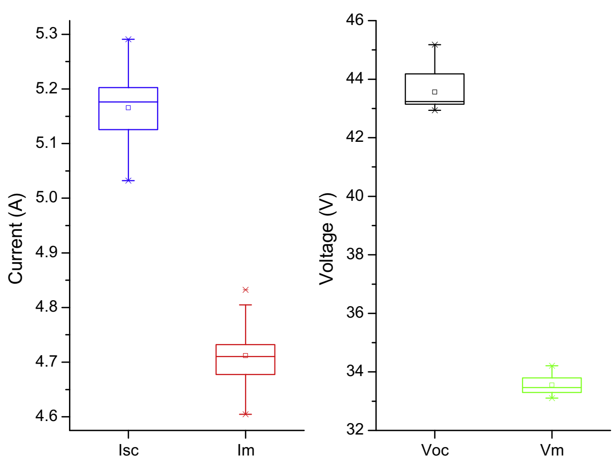

Fig. 8. Distribution of the converted I_{sc}, I_m, V_{oc} and V_m values to STC on 21st December 2012.

the manufacturer nameplate data of 5.43 A, and therefore, 5% of derating ratio for I_{sc} was taken into account. The determination procedure for V_{oc}, I_m and V_m derating factors is similar to that of I_{sc}. Finally, the derating factors and corrected values for the characteristic points are summarized in Table 4.

Based on the corrected specifications in Table 4, the parameters for the new simulation model in this study were recalculated (Table 5) and taken as a representative for all the modules in the system. A sample with derating factor and modified specification is presented in Fig. 7, which reveals that the predicted curve from the model with modified values is much more accurate than that with the manufacturer issued data.

6.3. PV model validation

To validate the new simulation model, comparisons between the field measurements and the calculated results were carried out for three cases: (1) one single PV module; (2) PV string with 9 modules connected in series; (3) PV array configured with 9 modules in series and 2 strings in parallel. All these measured items are shown in Fig. 6.

Table 4
Comparisons between specifications under STC and corrected values with derating factor.

	Manufacturer value at STC	Corrected value at STC	Derating factor (%)
I_{sc} (A)	5.43	5.16	5
V_{oc} (V)	44.6	43.7	2
I_m (A)	4.95	4.7	5
V_m (V)	35.4	33.6	5
Pmpp (W)	175	158	10

Table 5
Calculated parameter values with corrected values for PV cell/module model.

	I_{ph} (A)	I_o (A)	R_s (Ω)	R_p (Ω)	V_t (V)	n (deduced from V_t)
Cell	5.182	1.43E−09	0.0136	3.14	0.0276	1.075
Module	5.182	1.43E−09	0.9800	226.30	0.0276	1.075

6.3.1. Case I: one single module

The PV module M1, taken as an example, was employed to validate the modeling results for a single PV module. Fig. 9 present the I–V curves and P–V curves, respectively, for four different operating conditions with solar radiation from 235 W/m^2 to 870 W/m^2. It can be seen that the measured curve (red dashed line) and predicated curve from the modified model curve (black solid line) are very consistent. Very slight difference was observed only in #1 curve.

The environmental conditions, collected and simulated three characteristic points, deviations, as well as the time and date of each experiment, are summarized in Table 6. Fig. 9 and Table 6 highlight that the characteristic points from the simulation model are very close to the collected data.

As stated early, the modified model is only based on the preliminary measurements on the model M1. To validate the model for other modules, the I–V curves of other modules M1, M2, M3 and M4 were measured and compared with the calculated curve at the solar radiation of 840 W/m^2 (Fig. 10). It was found that predicted curve and all the measured curves have a high degree of consistency at short circuit point. Slight difference can be detected in curve of M2, especially at open circuit point and maximum power point. This phenomenon may result from different V_{oc} derating factor and specific V_{oc} temperature coefficient for M2, since these parameters can vary slightly from module to module.

6.3.2. Case II: PV string (S1)

The second case focuses on the PV string model validation. As revealed in Fig. 11, the proposed model

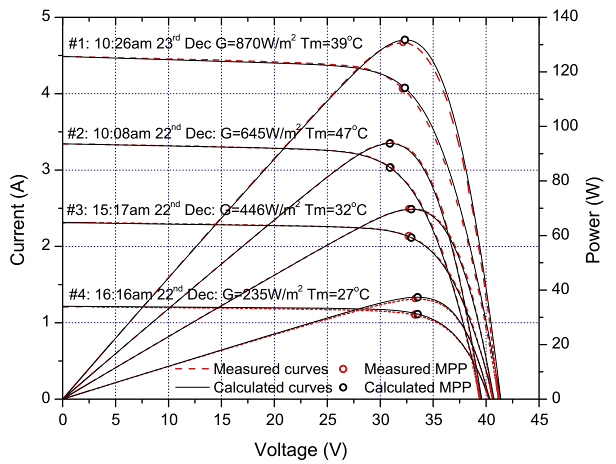

Fig. 9. Comparison between measured and calculated *I–V* curves, *P–V* curves and MPPs of PV module #M1.

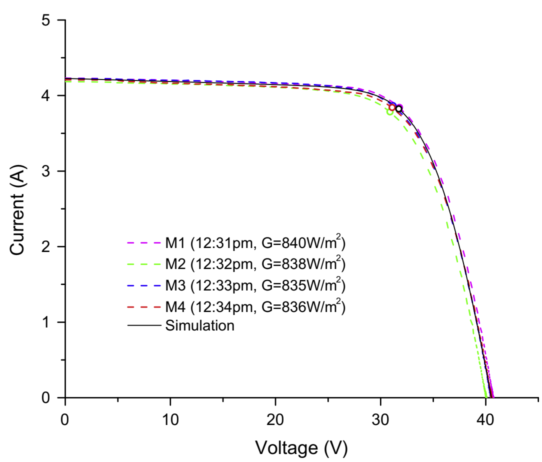

Fig. 10. *I–V* curves and MPP comparison between PV module #M1, #M2, #M3 and #M4.

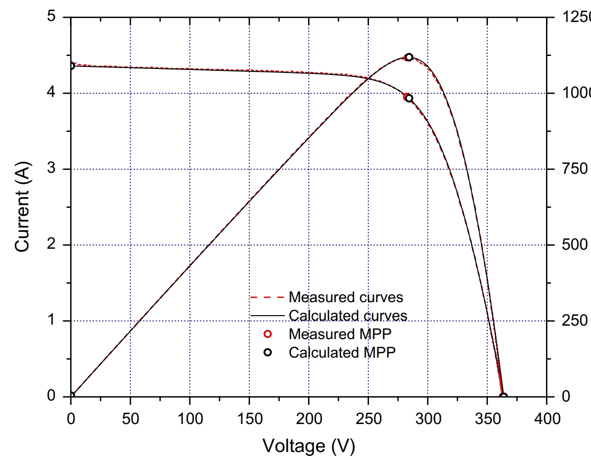

Fig. 11. Comparison between measured and calculated *I–V* curves, *P–V* curves and MPPs of PV string #S1.

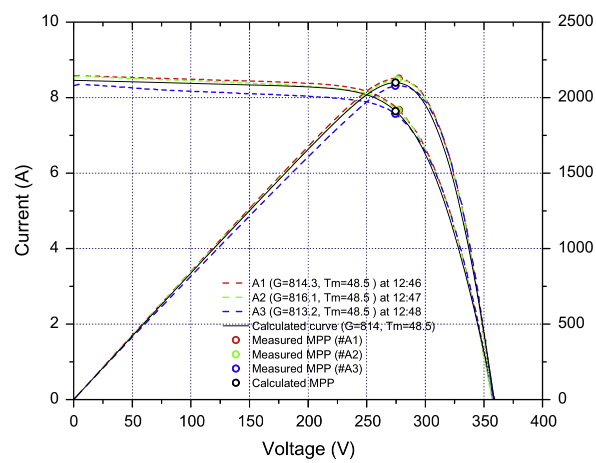

Fig. 12. Comparison between measured and calculated *I–V* curves, *P–V* curves and MPPs of PV array #A1, # A2, #A3.

demonstrates a very good agreement with the measured data both in current and power curves, as expected. The difference between the simulated Pmpp (1118.6 kW) and collected Pmpp (1116.8 W) is smaller than 0.5%. The practically null errors for the characteristic points demonstrate that the proposed model is very superior.

6.3.3. Case III: PV array (A1, A2, A3)

Finally, three PV subarrays A1, A2 and A3 were studied for array model validation. Once again, the A1 and A2 simulation results presented in Fig. 12 match well with the measured data. The difference existing in A3 possibly

Table 6
The characteristic points (I_{sc}, V_{oc} and Pmmp) comparisons between PV module #M1's measured data and calculated data.

Test no.	Time and date	Solar radiation (W/m^2)	Module temp. (°C)	Amb. temp (°C)	I_{sc} (A)			V_{oc} (V)			Pmpp (W)		
					Meas.	Cal.	Devi. (%)	Meas.	Cal.	Devi. (%)	Meas.	Cal.	Devi. (%)
#1	10:26 23/12/2012	870	39	20	4.49	4.49	0.0	41.22	41.39	0.4	130.72	131.75	0.8
#2	10:08 22/12/2012	645	47	24	3.34	3.34	0.1	39.42	39.58	0.4	93.83	93.76	−0.1
#3	15:17 22/12/2012	446	32	23	2.31	2.31	−0.2	40.66	40.75	0.2	69.78	69.64	−0.2
#4	16:16 22/12/2012	235	27	20	1.21	1.22	0.9	40.34	40.33	0.0	36.85	37.36	1.4

results from slight shading from PV string S1 at that time or other defects (such as hotspots) in A3. To have a further defects inspection, more measurements should be conducted in the future. Anyway, the discrepancy between the maximum power point of three arrays and simulation data is very small.

From the figures above (Figs. 9–12), basically all the measured curves and the predicted curves from the module/string/array model with derating factor are very similar under different operating conditions. In addition, some defects or mismatch in the existing system can be detected by using the developed model. The perfect agreement between the calculated and measured results, both in the *I–V* curves and characteristic points, demonstrates the reliability and accuracy of the simulation model. In addition, the experimental data was continuously collected by the research group for different seasons to validate the long term performance of this model. The effect of implementing more *I–V* curve measurements throughout the year on the accuracy of the results will be discussed in our future research.

7. Conclusions

A novel theoretical model in the Matlab for determining the performance parameters of PV modules/strings/arrays was developed in this paper. The feasibility of the proposed model was firstly demonstrated by comparing the predicted results with those from other software and models. Validation of the simulation model was performed through the comparison between simulation results and measurements from a real grid-connected PV system in Hong Kong under different irradiance and temperature conditions. However, the behavior of the model with the manufacturer issued data cannot match the real operating performance under real weather conditions because the system was subjected to soiling, aging and/or other degradation factors. Therefore, a suitable modification to the model with reasonable derating factor has been proposed for a PV system. The new model with derating factor is very superior, and very high degree of consistency can be observed between the collected and predicted data, especially around the characteristic points, which can demonstrate its high-accuracy and feasibility.

This new approach enables engineers to calculate the performance parameters by using the specifications provided by PV manufacturer only, offering a good compromise between simplicity and accuracy. Besides, the simulation model can be used to precisely model the *I–V* relationships for PV cell/module/string/array at any solar irradiance and temperatures, especially around the characteristic points. This reliable simulation model can, therefore, be very helpful for designers and engineers to accurately determine the characteristic curves and operating performance of any PV module/string/array.

Acknowledgements

The work described in this paper is financially supported by The Hong Kong polytechnic University and China Light & Power (CLP) Holding Limited (Hong Kong).

References

Ahmad, G.E., Hussein, H.M.S., El-Ghetany, H.H., 2003. Theoretical analysis and experimental verification of PV modules. Renew. Energy 28, 1159–1168.

Almonacid, F., Rus, C., Hontoria, L., Muñoz, F.J., 2010. Characterisation of PV CIS module by artificial neural networks. A comparative study with other methods. Renew. Energy 35, 973–980.

Bellini, A., Bifaretti, S., Iacovone, V., Cornaro, C., 2009. Simplified model of a photovoltaic module. Appl. Electron., 47–51.

Benlarbi, K., Mokrani, L., Nait-Said, M.S., 2004. A fuzzy global efficiency optimization of a photovoltaic water pumping system. Sol. Energy 77, 203–216.

Blas, M.A.d., Torres, J.L., Prieto, E., García, A., 2002. Selecting a suitable model for characterizing photovoltaic devices. Renew. Energy 25, 371–380.

Carrero, C., Amador, J., Arnaltes, S., 2007. A single procedure for helping PV designers to select silicon PV modules and evaluate the loss resistances. Renew. Energy 32, 2579–2589.

Celik, A.N., Acikgoz, N., 2007. Modelling and experimental verification of the operating current of mono-crystalline photovoltaic modules using four- and five-parameter models. Appl. Energy 84, 1–15.

Chan, D.S.H., Phang, J.C.H., 1987. Analytical methods for the extraction of solar-cell single- and double-diode model parameters from *I–V* characteristics. IEEE Trans. Electron Dev. 34, 286–293.

De Soto, W., Klein, S.A., Beckman, W.A., 2006. Improvement and validation of a model for photovoltaic array performance. Sol. Energy 80, 78–88.

Dongue, S.B., Njomo, D., Tamba, J.G., Ebengai, L., 2012. Modeling of electrical response of illuminated crystalline photovoltaic modules using four- and five-parameter models. Int. J. Emerging Technol. Adv. Eng. 2, 612–619.

Durisch, W., Tille, D., Wörz, A., Plapp, W., 2000. Characterisation of photovoltaic generators. Appl. Energy 65, 273–284.

Gow, J.A., Manning, C.D., 1999. Development of a photovoltaic array model for use in power-electronics simulation studies. IEEE Proc. Power Appl. 146, 193–200.

Hadj Arab, A., Chenlo, F., Benghanem, M., 2004. Loss-of-load probability of photovoltaic water pumping systems. Sol. Energy 76, 713–723.

Hansen, A.D., Sørensen, P., Hansen, L.H., Bindner, H., 2000. Models for a Stand-Alone PV System. Risø National Laboratory, pp. 77.

INSEL software: <http://www.insel.eu/> (last accessed on 26.06.13).

Ishaque, K., Salam, Z., 2011. An improved modeling method to determine the model parameters of photovoltaic (PV) modules using differential evolution (DE). Sol. Energy 85, 2349–2359.

Ishaque, K., Salam, Z., Taheri, H., 2011a. Simple, fast and accurate two-diode model for photovoltaic modules. Sol. Energy Mater. Sol. Cells 95, 586–594.

Ishaque, K., Salam, Z., Taheri, H., Shamsudin, A., 2011b. A critical evaluation of EA computational methods for photovoltaic cell parameter extraction based on two diode model. Sol. Energy 85, 1768–1779.

Jäger-Waldau, A., 2012. PV Status Report 2012. Joint Research Centre (European Commission).

Karatepe, E., Boztepe, M., Colak, M., 2006. Neural network based solar cell model. Energy Convers. Manage. 47, 1159–1178.

Kim, S.-K., Jeon, J.-H., Cho, C.-H., Kim, E.-S., Ahn, J.-B., 2009. Modeling and simulation of a grid-connected PV generation system for electromagnetic transient analysis. Sol. Energy 83, 664–678.

King, D.L., Kratochvil, J.A., Boyson, W.E., 2004. Photovoltaic array performance model. Sandia National, Laboratories, Dept. of, Energy, United States, Washington, D.C., Oak Ridge, Tenn.

Lo Brano, V., Orioli, A., Ciulla, G., Di Gangi, A., 2010. An improved five-parameter model for photovoltaic modules. Sol. Energy Mater. Sol. Cells 94, 1358–1370.

Lo Brano, V., Orioli, A., Ciulla, G., 2012. On the experimental validation of an improved five-parameter model for silicon photovoltaic modules. Sol. Energy Mater. Sol. Cells 105, 27–39.

Mellit, A., Benghanem, M., Kalogirou, S.A., 2007. Modeling and simulation of a stand-alone photovoltaic system using an adaptive artificial neural network: proposition for a new sizing procedure. Renew. Energy 32, 285–313.

Meyer, E.L., van Dyk, E.E., 2000. Development of energy model based on total daily irradiation and maximum ambient temperature. Renew. Energy 21, 37–47.

Muneer, T., Asif, M., Kubie, J., 2003. Generation and transmission prospects for solar electricity: UK and global markets. Energy Convers. Manage. 44, 35–52.

PVsyst software: <http://www.pvsyst.com/> (last accessed on 26.06.13).

PVWATTS software: <http://www.nrel.gov/rredc/pvwatts/> (last accessed on 26.06.13).

Saloux, E., Teyssedou, A., Sorin, M., 2011. Explicit model of photovoltaic panels to determine voltages and currents at the maximum power point. Sol. Energy 85, 713–722.

Sera, D., Teodorescu, R., Rodriguez, P., 2007. PV panel model based on datasheet values. In: IEEE International Symposium on Industrial Electronics ISIE 2007. pp. 2392–2396.

Tian, H., Mancilla-David, F., Ellis, K., Muljadi, E., Jenkins, P., 2012. A cell-to-module-to-array detailed model for photovoltaic panels. Sol. Energy 86, 2695–2706.

Walker, G., 2001. Evaluating MPPT converter topologies using a matlab PV model. J. Elect. Electron. Eng. Australia 21, 49–55.

Zhang, L., Al-Amoudi, A., Yunfei, B., 2000. Real-time maximum power point tracking for grid-connected photovoltaic systems. In: Eighth International Conference on Power Electronics and Variable Speed Drives IEEE Conf. Publ. No. 475, pp. 124–129.